Response of stratospheric circulation and stratosphere-troposphere exchange to changing sea surface temperatures

Mark A. Olsen,[1] Mark R. Schoeberl,[2] and J. Eric Nielsen[3]

Received 8 September 2006; revised 19 May 2007; accepted 5 June 2007; published 21 August 2007.

[1] The Goddard Earth Observing System, version 4 general circulation model (GCM) is used to examine the influence of sea surface temperatures (SSTs) on stratospheric circulation and extratropical stratosphere-troposphere exchange (STE). The simulation uses observed SSTs from 1949 to 1998 at the lower boundary. The atmospheric greenhouse gas (GHG) burden is interannually constant to artificially decouple the radiative influence from the SST forcing. A stronger SST gradient from the tropics through the middle latitudes results in a greater meridional temperature gradient in the subtropical troposphere. The upper tropospheric zonal winds increase consistent with the thermal wind relationship, and vertically propagating waves are refracted more poleward into the stratosphere. As a consequence, the stratospheric residual circulation is strengthened. This is manifest as a net annual mass STE increase of 2.7% per decade in the Northern Hemisphere and 2.0% per decade in the Southern Hemisphere. Likewise, the characteristic residence time of air in the lowermost stratosphere decreases by about a month. The STE trends and upper tropospheric temperature gradients are not significantly different in a second simulation that specifies an increasing GHG burden. The second simulation also shows that the radiative cooling from an increased GHG burden is greater in magnitude than the SST-induced dynamical warming in the polar stratosphere. The results of this study imply that the modeled circulation of the stratosphere can be significantly affected by the SSTs. It follows that the fidelity of simulations of the 21st century atmosphere strongly depends on the SSTs, whether prescribed or interactive.

Citation: Olsen, M. A., M. R. Schoeberl, and J. E. Nielsen (2007), Response of stratospheric circulation and stratosphere-troposphere exchange to changing sea surface temperatures, *J. Geophys. Res.*, *112*, D16104, doi:10.1029/2006JD008012.

1. Introduction

[2] The rate of stratosphere-troposphere exchange (STE) of mass and constituents at midlatitudes is critical to the chemistry of both regions. Trace gases primarily produced in the stratosphere, such as ozone and hydrogen chloride, have relatively rapid loss rates in the troposphere. The ozone flux is an important boundary condition determining the oxidizing capacity of the troposphere [*Levy*, 1971]. In addition, ozone and other greenhouse gases (GHGs) in the upper troposphere/lower stratosphere significantly impact the radiative balance of the atmosphere [e.g., *Haywood et al.*, 1998]. Any trend in the rate of STE would directly or indirectly contribute to observed trends in stratospheric trace gases. *Butchart and Scaife* [2001] illustrate that increasing the rate of STE accelerates the removal of ozone-destroying CFCs from the atmosphere, decreasing the time of ozone recovery estimates.

[3] The Brewer-Dobson circulation qualitatively describes the large-scale exchange between the stratosphere and troposphere [*Brewer*, 1949; *Dobson*, 1956]. Air rises into the stratosphere in the tropics and descends at higher latitudes. Wave dissipation in the stratosphere forces the poleward transport [*Hoskins*, 1991; *Holton et al.*, 1995] and ultimately drives the net poleward and downward residual circulation [e.g., *Andrews et al.*, 1987]. *Haynes et al.* [1991] show that more wave driving occurs in the Northern Hemisphere (NH) than the Southern Hemisphere (SH) as a result of greater orographic variability. The net extratropical STE of mass is likewise estimated to be on the order of 10% greater in the NH [e.g., *Appenzeller et al.*, 1996; *Schoeberl*, 2004].

[4] Model studies have shown that changes in the composition of the atmosphere can force changes in the stratospheric circulation. The residual circulation has been shown to consistently strengthen in response to GHG-induced climate change in a wide range of general circulation models (GCMs) [*Rind et al.*, 1990; *Butchart and Scaife*, 2001; *Sigmond et al.*, 2004; *Butchart et al.*, 2006]. These studies show that globally the troposphere warms and the stratosphere cools in response to increased CO_2. The studies also agree that increasing wave dissipation in the stratosphere forces the change in the circulation. However, the details of the attributed mechanism and response are varied.

[1]Goddard Earth Sciences and Technology Center, University of Maryland Baltimore County, Baltimore, Maryland, USA.
[2]NASA Goddard Space Flight Center, Greenbelt, Maryland, USA.
[3]Science Systems and Applications, Inc., Lanham, Maryland, USA.

Copyright 2007 by the American Geophysical Union.
0148-0227/07/2006JD008012

Rind et al. [1990] ran several simulations of a GCM with doubled CO_2 to show that there was more longwave propagation from the troposphere and that the refractive properties were altered because of a greater latitudinal temperature gradient in the lower stratosphere. While one simulation resulted in more poleward refraction and another had more equatorward refraction, more eddy energy in the stratosphere in both simulations resulted in a stronger residual circulation. Other studies show that altered refraction does not play a role in or is not a necessity for increasing the circulation [*Butchart and Scaife*, 2001; *Eichelberger and Hartmann*, 2005].

[5] Most model studies agree that increasing the CO_2 burden results in more wave propagation from the troposphere [e.g., *Butchart and Scaife*, 2001; *Eichelberger and Hartmann*, 2005; *Butchart et al.*, 2006]. However, *Sigmond et al.* [2004] note that there is an increase in the vertical wave propagation just above the winter tropopause, yet there is a decrease in the tropospheric wave activity in their simulation. They suggest that either more wave activity is generated near the tropopause or that the tropopause becomes more permeable to waves propagating from the troposphere. In greater contrast a simulation by *Langematz et al.* [2003] includes the radiative effects of ozone depletion with CO_2 increases and show a decrease in planetary wave activity in the stratosphere with a corresponding reduction in the residual circulation.

[6] Sea surface temperatures (SSTs) are linked to the atmospheric GHG burden. Observed warming trends in tropical SSTs are at least partly due to increased GHGs [*Knutson and Manabe*, 1998; *Knutson et al.*, 1999]. However, SST changes can impact the dynamics of the atmosphere and climate, extending into the stratosphere. *Hoerling et al.* [2001] demonstrate that tropical SSTs are linked to the North Atlantic climate and that warmer tropical SSTs force a trend toward one extreme phase of the North Atlantic Oscillation. *Grassi et al.* [2005] show that a trend in tropical SST may influence SH polar dynamics, delay the vortex breakup, and contribute to Antarctic climate changes. Given the results of these studies, it is reasonable to hypothesize that SST trends may impact stratospheric wave activity responsible for driving the stratospheric residual circulation. Indeed, *Rind et al.* [1990] illustrate that the magnitude and structure of the SST field does affect the amount of eddy energy in the stratosphere as well as the spatial distribution of the eddy energy.

[7] The present study examines the impact of SST changes on the stratospheric residual circulation and STE. The influence is isolated from direct radiative mechanisms by holding the GHG boundary conditions constant in the GCM radiation scheme while using observed SST fields from 1949 to 1998. Section 2 describes the model and simulation. The results are presented in section 3 and are followed by a discussion and conclusions in sections 4 and 5, respectively.

2. Model and Simulations

[8] In section 3 we examine two 50-year simulations using the Goddard Earth Observing System, version 4 (GEOS-4) GCM (described in *Bloom et al.* [2005]). The GCM is run at a horizontal resolution of $2.5° \times 2°$ and spans 55 vertical levels up to 0.01 hPa. The ability of the GEOS-4 GCM to reproduce the stratospheric circulation has been well documented. The age of air and residual circulation of the GEOS-4 GCM have been shown to be reasonable and more realistic than assimilated data sets [*Schoeberl et al.*, 2003]. *Douglass et al.* [2003] used the meteorological fields from an earlier version of the GEOS-4 GCM to drive the Goddard Space Flight Center (GSFC) chemistry and transport model (CTM). They demonstrated that the large-scale stratospheric transport is well reproduced compared to observations. Meteorological fields from the GCM simulations of the present work have been used to drive the GSFC CTM in several previous studies. *Olsen et al.* [2004] used 5 early years of the simulation to demonstrate that the STE of mass and ozone compares well with observational-based estimates. *Stolarski et al.* [2006] show that derived trends in ozone can be significantly affected by the interannual variability of the stratospheric dynamics. The GCM and CTM outputs have also been used to illustrate a method of detecting climatological changes in the residual circulation [*Olsen et al.*, 2006].

[9] In the present study, one simulation, defined as Run O (for observed SSTs), specifies the Met Office Hadley Centre monthly mean observed SSTs and ice cover from 1949 to 1998 [*Rayner et al.*, 2003]. The SSTs are linearly interpolated from month to month to provide a smoothly varying field. Run C (for climatological SSTs) uses annually repeating climatological monthly means of the observed SSTs. All other boundary conditions and specifications of the two simulations are identical. The specified concentrations of radiatively important gases have a seasonal dependence but do not vary interannually, held at approximate 1992 levels. These specified gases include CO_2, CH_4, N_2O, CFC-11, and CFC-12. We note that the observed sea surface temperatures are ultimately forced by the changes in the atmospheric loading of these gases. Therefore these simulations indirectly include the trend in GHGs as expressed through the SSTs. This decoupling approach is not physically realistic. However, it is useful to isolate the influence of the SSTs on the atmospheric dynamics and determine if the SST forcing may play a role in strengthening the Brewer-Dobson circulation.

[10] Throughout much of the present study, we refer to a "decadal-mean difference" to illustrate changes and trends of quantities in Run O. We define this to be the mean of the first decade subtracted from the mean of last decade. The decadal-mean difference of the annual mean SSTs used in Run O is shown in Figure 1. The net global change is +0.18 K. The net changes are +0.24 and +0.11 K in the NH and SH, respectively. Nearly all the tropical oceans are warmer in the last decade compared with the first decade; however, large regions in the extratropics are cooler. These cooler regions are greater in area and magnitude in the NH than the SH. The majority of the North Atlantic becomes cooler, as does a large pool centered on the dateline in the North Pacific. There is also a region of cooler SSTs at the dateline in the SH but no corresponding cool region exists in the South Atlantic.

3. Results

[11] We have calculated the annual net extratropical STE of mass for both simulations using the mass balance

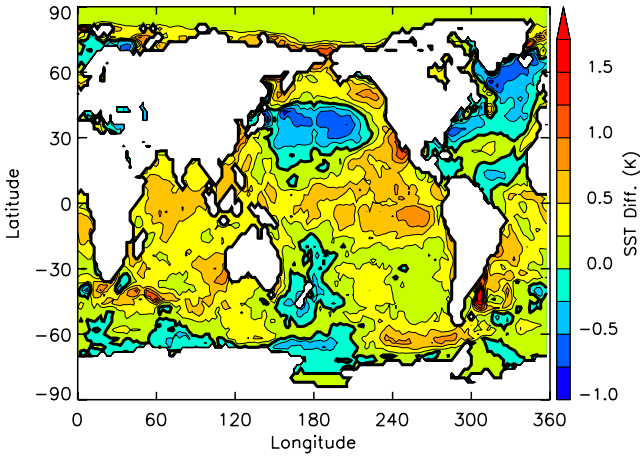

Figure 1. Decadal-mean difference (see text) of annual SST. Bold lines are the zero contours. Blues (greens to reds) are negative (positive) differences. Contour interval is 0.25 K.

diagnostic introduced by *Appenzeller et al.* [1996]. In this diagnostic the STE is determined as the sum of the flux across the 380 K surface and the time rate of change of mass between the tropopause and 380 K surface, the lowermost stratosphere. The tropopause is chosen as the 3.5 potential vorticity unit (PVU) surface (1 PVU = 10^{-6} m^2 K kg^{-1} s^{-1}) [*Schoeberl*, 2004]. The 380 K flux is computed using the net heating rate fields that are outputs of the GCM. The net downward extratropical tropopause flux equals the net upward flux across the tropical tropopause over a long time average. The accuracy of an annual STE estimate using this diagnostic depends upon the heating rate fields rather than the wind fields and trajectory schemes used by Lagrangian methods of STE estimation. In our simulations the annual mean mass of the lowermost stratosphere remains constant so the annual mass flux is ultimately determined by the flux across the 380 K surface. Thus the choice of the tropopause definition is irrelevant to the trends discussed.

[12] Figure 2 shows the annual extratropical mass STE with a least squares fit, negative values indicate net mass transport from the stratosphere to the troposphere. Run O exhibits an increasing trend of 2.7 ± 0.5% per decade in the NH and 2.0 ± 0.6% per decade in the Southern Hemisphere (SH). The Run C STE trends are 0.03 ± 0.3% per decade and 0.2 ± 0.4% per decade in the NH and SH, respectively. The error estimates are 1σ uncertainties. The Run O trends are at least an order of magnitude greater than the trends in the control Run C for both hemispheres. In addition, the trends are statistically significant at greater than 99% confidence in Run O while the Run C trends are not significantly different from zero. However, the interannual variability of the STE is great enough that the Run O trend difference between the NH and SH is not significant.

[13] As we will demonstrate in this section, the STE trends are a consequence of large-scale changes to the atmospheric dynamics and circulation. The SSTs are the only boundary condition differences of the two simulations and must be the source of the STE trend. Since *Rind et al.* [1990] demonstrate that the stratospheric eddy kinetic energy and residual circulation are sensitive to the latitudinal SST gradient, we try to find a similar connection between STE and the SST gradient. We show in Figure 3 that the annual STE in Run O significantly correlates with the difference of the middle latitude zonal mean SST and the tropical (NH) or subtropical (SH) zonal mean SST. A greater SST difference is associated with more transport from the extratropical stratosphere to the troposphere. The NH STE is most significantly correlated with the SST difference between the 0–10°N and 30–40°N zonal mean bands (r = 0.62). The latitudes that most impact the SH STE magnitude are shifted more poleward than in the NH. The strongest correlation exists with the difference between the 20–30°S and 50–60°S zonal mean bands (r = 0.33). This correlation is much weaker than in the NH, though it is still significant at greater than 95% confidence.

[14] The NH STE also correlates nearly as significantly with the mean temperature between 30–40°N. This corresponds to the large, colder regions in both the Atlantic and Pacific Oceans. A significant correlation of STE to any

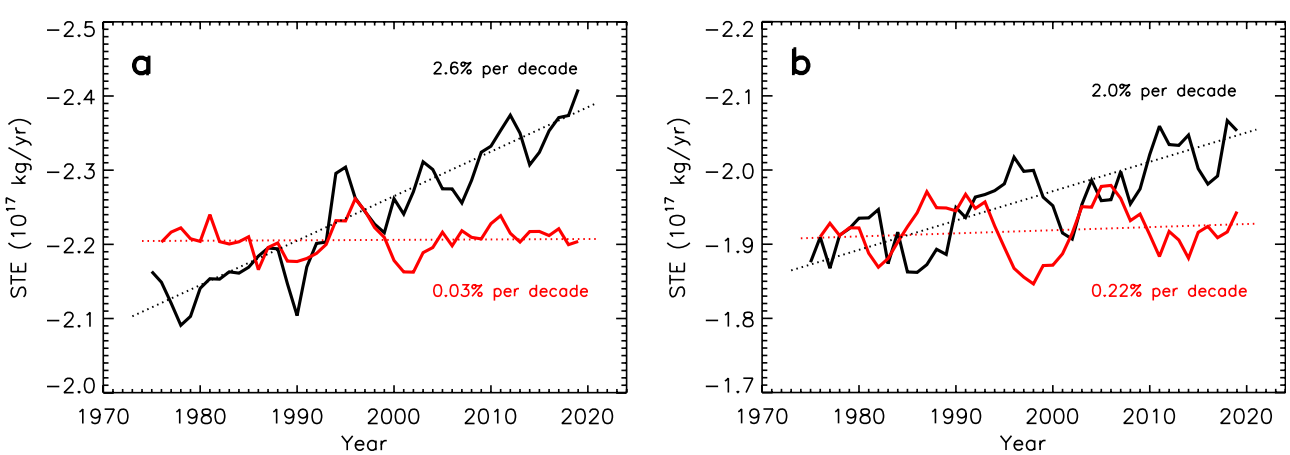

Figure 2. Annual extratropical mass STE for (a) the NH and (b) the SH. Black lines are results from Run O (observed SSTs), and red lines are from Run C (climatological mean SSTs). Negative values indicate net stratosphere to troposphere transport. Results shown are smoothed with a 5-year mean. Trend calculated using least squares fitting to the unsmoothed results.

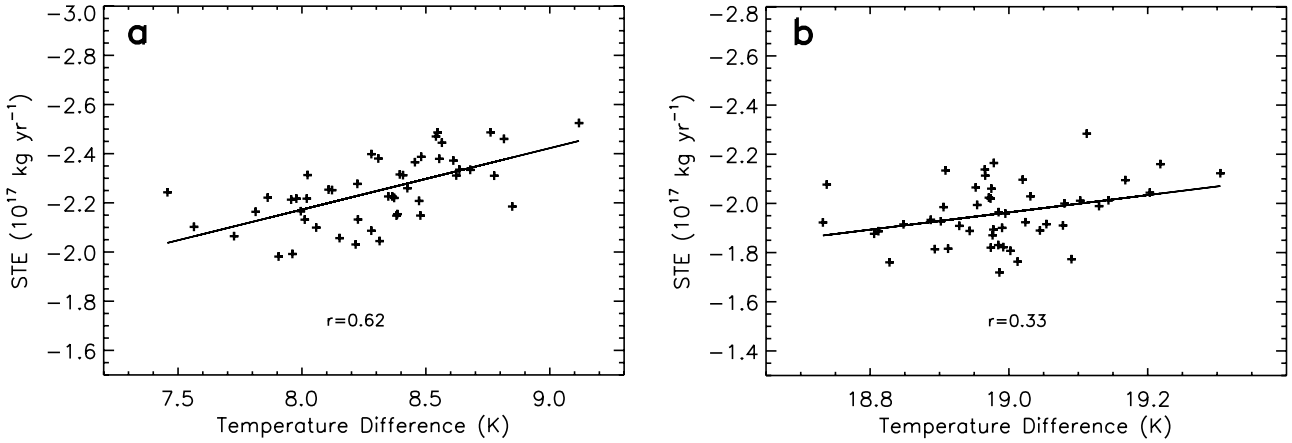

Figure 3. Correlation of annual extratropical STE with the difference of two zonal mean SSTs. (a) The NH STE versus the SST difference between the 0°–10°N and 30°–40°N zonal mean bands. (b) The SH STE versus the SST difference between the 20°–30°S and 50°–60°S zonal mean bands.

simple 10° latitude band does not exist in the SH. The less zonally symmetric cooler SSTs in the SH may account for this. However, the actual NH asymmetric forcing may be greater in the NH because of land-sea contrasts. Thus to determine the cause of the weaker SH STE-SST correlation requires further study.

[15] In the remainder of this section we examine the changes to the temperature, wind structure, and associated dynamics in Run O. The changes to the stratospheric residual circulation are resolved as well as the mechanism for the STE trend. We restrict most of our discussion to the NH for brevity. The wave activity is strongest in winter so we highlight the December–February (DJF) rather than annual means. The SH winter characteristics are similar but less prominent and shifted poleward in the SH compared to the NH.

[16] The decadal-mean difference of the DJF zonal mean temperature is shown in Figure 4. The standard error of the decadal-mean DJF temperature is computed at all latitudes and altitudes for both decades. Significant decadal-mean differences exist where the magnitude of the difference is greater than the sum of both decadal uncertainties. These regions are shown without cross-hatching in Figure 4. The DJF zonal mean dynamical tropopause and 380 K potential temperature surface averaged over the entire run are also depicted. There is no trend in the heights of these surfaces. This agrees with no long-term changes in the annual mean mass between these surfaces (the lowermost stratosphere), as previously noted. The temperature structure of warmer and cooler regions in the stratosphere is consistent with a stronger Brewer-Dobson circulation. The NH extratropical stratosphere tends to be warmer by the end of the simulation. The SH polar stratosphere is also warmer but, unlike much of the NH extratropics, it is not statistically significant during DJF. The tropical stratosphere is cooler by the end of the simulation with the greatest decrease occurring near the stratopause. We note that the global mean temperature of the middle and upper stratosphere does not change. The global area-weighted mean temperature change at each level at and above 70 hPa is not significantly different from zero. This suggests that the zonal mean temperature differences in the stratosphere result from changes in the dynamical forcing.

[17] Most of the troposphere increases in temperature except for regions in the extratropical NH where the changes are not significant. The greatest tropospheric warming occurs in the tropical upper troposphere. The location of the maximum is similar to results of previous studies that explicitly include the radiative impact of increased CO_2 [*Rind et al.*, 1990, 1998; *Mahfouf et al.*, 1994; *Sigmond et al.*, 2004]. The simulation exhibits greater heating from moist processes in the upper troposphere at the equator during the later decade. The warmer tropical SSTs increase the effective potential temperature at the surface, shifting the moist adiabat. The tropical atmosphere in the model readjusts to neutral stability via increased convection, leading to warmer upper tropospheric temperatures.

[18] The DJF decadal-mean difference of the mean zonal winds is shown in Figure 5. The winds become stronger in

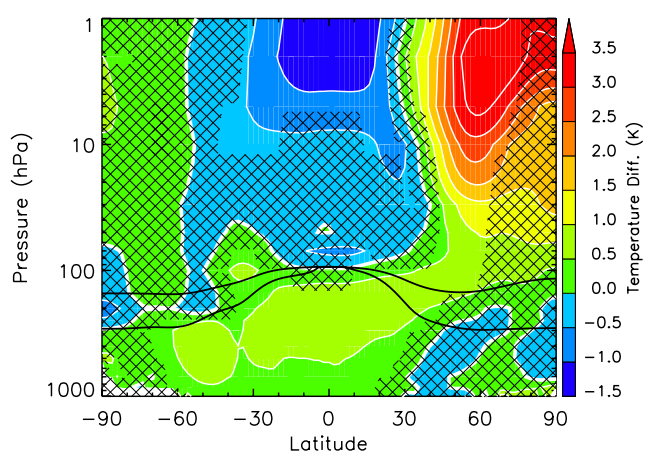

Figure 4. Decadal-mean difference of the DJF zonal mean temperature. Blues (greens to reds) are negative (positive) differences. Contour interval is 0.5 K. Bold white lines are the zero contours. Cross-hatching denotes regions where the differences are not statistically significant. The quasi-horizontal black lines indicate the mean DJF tropopause and 380 K surface where the tropopause is the lower of the two lines in the extratropics.

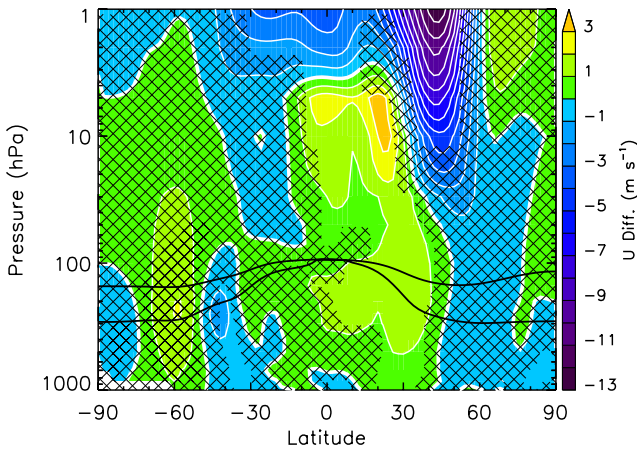

Figure 5. Decadal-mean difference of the DJF zonal wind. Purples to blues (greens to yellows) are negative (positive) differences. Contour interval is 1 m s^{-1}. Bold white lines are the zero contours. Cross-hatching denotes regions where the differences are not statistically significant. The quasi-horizontal black lines indicate the mean DJF tropopause and 380 K surface where the tropopause is the lower of the two lines in the extratropics.

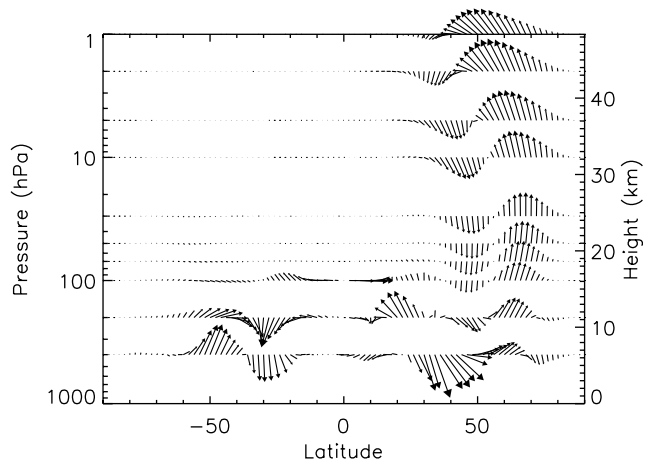

Figure 6. Decadal-mean difference of the DJF EP flux. The flux has been multiplied by the cosine of latitude. The vectors are plotted such that 7.8 × 10^6 kg s^{-2} is scaled to 10° latitude in the horizontal and 7.1 × 10^6 kg s^{-2} is scaled to 10 km in the vertical.

the upper troposphere/lower stratosphere equatorward of about 50°N because of the greater horizontal temperature gradient. There is also a significant weakening of the upper stratospheric jet equatorward of 60°N consistent with the changes to the temperature gradient there. The change to the wind field in the upper stratosphere results in an ~3° northward shift of the climatological location of the jet.

[19] The vertical wave propagation is dependent on the strength of the zonal mean wind. Analogous to optical theory, the path of wave propagation is determined by an atmospheric index of refraction [e.g., *Andrews et al.*, 1987]. This index is dependent on the inverse of the zonal mean wind. Thus, given that all other factors are equal, propagating waves will prefer paths toward weaker westerly winds (higher indices of refraction) and away from stronger westerlies (lower indices). The decadal-mean difference of the DJF Eliassen-Palm (EP) flux is shown in Figure 6. Very little difference exists in the SH during the boreal winter when the wave propagation from the troposphere is an order of magnitude less than in the NH. A pattern of both negative and positive differences occurs through the NH stratosphere at the latitudes where the EP flux is greatest. At 100 hPa the differences in the vertical component changes sign at ~55°N, which is near where the wind differences also change sign. The differences in the vertical propagation equatorward of 40°N at 100 hPa are damped out near this level, while the signal of the poleward differences propagates through the entire stratosphere. Changes in the refraction of the wave propagation are indicated by the decadal-mean difference of the meridional component of the EP flux (Figure 7). Significant poleward changes to the meridional component exist in the later decade throughout the extratropical troposphere and lower stratosphere. There is a correspondence of where the tropospheric refraction occurs with the pattern of negative and positive changes in the vertical component of the extratropical stratospheric EP flux (Figure 6). This is consistent with waves of middle to lower tropospheric origin refracting more poleward in the upper troposphere/lowermost stratosphere and entering the stratosphere above 100 hPa at higher latitudes during the last decade compared with the first decade.

[20] Zonal forcing by wave dissipation, expressed as EP flux convergence, contributes to the transformed Eulerian mean residual circulation [e.g., *Andrews et al.*, 1987]. The decadal-mean difference of the DJF EP flux divergence is shown in Figure 8. There is greater convergence in the higher-latitude NH stratosphere, particularly in the upper stratosphere. The enhanced convergence corresponds to where there is increased vertical wave propagation (Figure 6) that results from the greater poleward refraction near the tropopause. The greater wave driving increases the poleward meridional circulation and hence the downwelling on

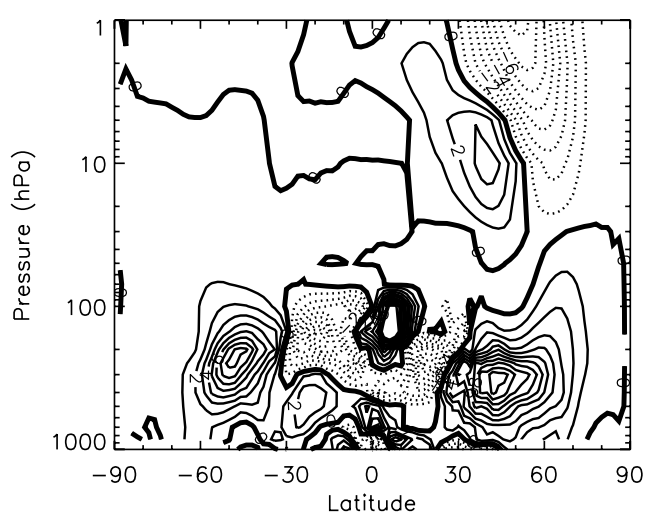

Figure 7. Decadal-mean difference of the meridional component of the DJF EP flux. The flux has been multiplied by the cosine of latitude. Values are scaled the same as Figure 6. Solid lines are positive contours, indicating a northward change.

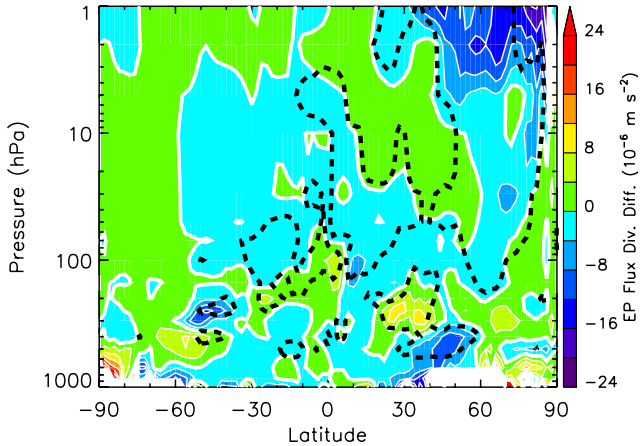

Figure 8. Decadal-mean difference of the EP flux divergence. Purples to blues (greens to reds) are negative (positive) differences. Contour interval is 4 m s^{-2}. Bold white lines are the zero contours. The dashed line denotes where the convergence and divergence is significantly correlated to the NH annual STE at greater than 95% confidence.

the poleward side of the convergence as stated by the downward control principle [*Haynes et al.*, 1991]. The decadal-mean difference of the residual circulation for DJF is shown in Figure 9. The full residual circulation stream function slightly ascends poleward in the stratosphere near 50°N, thus the later decade exhibits greater upward motion in this region, resulting in increased poleward transport near the stratopause in agreement with the change in EP flux convergence here. This meridional transport is balanced by more descent poleward of ~65°N through much of the stratosphere.

[21] We conclude the results by showing that the trend in the stratosphere to troposphere transport across the extratropical tropopause is linked to the changes in the stratospheric wave driving and residual circulation. A correlation coefficient is calculated comparing the annual time series of the DJF mean EP flux divergence at each model latitude and altitude with the NH annual STE that is shown in Figure 2. The dashed line in Figure 8 shows where the magnitude of the annual NH STE time series is correlated to the convergence and divergence of the annual DJF mean EP flux time series at greater than 95% confidence. In particular, the correlation exists through most of the extratropical NH, including the upper stratosphere where the greatest changes in the wave driving exist. The greatest stratospheric wave driving occurs during the winter months and the corresponding EP flux divergence changes are also greatest during this time. During the other seasons, no coherent pattern of significant correlation exists between the NH STE and the EP flux convergence and divergence.

4. Discussion

[22] The STE trend in Run O compares well with the global trend of 3% per decade found by *Butchart and Scaife* [2001] using a version of the Met Office Unified Model. *Butchart et al.* [2006] show that the mean global trend from a comparison of many models was about 2% per decade. These studies explicitly include the heating rate changes from trends in GHGs. The present study shows that an STE trend of similar magnitude can be forced solely by changes in SSTs. Direct radiative changes to atmospheric temperatures by an increasing GHG load are not a necessity for increasing STE and the residual circulation.

[23] We examine a 34-year simulation to investigate how explicit GHG changes would change our results. This 1950–1983 simulation is identical to Run O, using the same SSTs, except that it includes an increasing atmospheric burden of CO_2 in the radiation scheme. The atmospheric CO_2 concentration increases by about 10% over the length of the run. In this simulation, which we will refer to as Run G, the STE increases by 1.0 ± 0.7% per decade and 2.4 ± 0.7% per decade in the NH and SH, respectively. Over the same time span the STE in Run O increases by 2.1 ± 0.9% per decade in the NH and 1.2 ± 1.0% per decade in the SH. The differences of the trends are not significant when comparing the two simulations. The stratosphere cools globally with time in Run G, concurring with previous studies [*Rind et al.*, 1990; *Butchart and Scaife*, 2001; *Sigmond et al.*, 2004; *Butchart et al.*, 2006]. Below 100 hPa and equatorward of 60° the DJF NH decadal-mean temperature difference in Run G is very similar to the Run O results over the same time span in both magnitude and structure. In both cases the temperature gradient becomes greater. Accordingly, the changes in the wind field in this region are also comparable between the two runs. The similarity of these results indicates that the SST-induced dynamical changes play a significant role in changing the residual circulation and STE.

[24] Studies that explicitly increase the GHG burden exhibit a global cooling of the stratosphere. We previously noted that this contrasts with the warming trend in the polar stratosphere exhibited by Run O. However, in our Run G the global stratosphere above 100 hPa becomes cooler with time with the exception of slight warming in the lower stratosphere near 60°S. *Eichelberger and Hartmann* [2005] used a simple GCM on a sphere with no changing surface temperatures and a tropical tropospheric heating source to

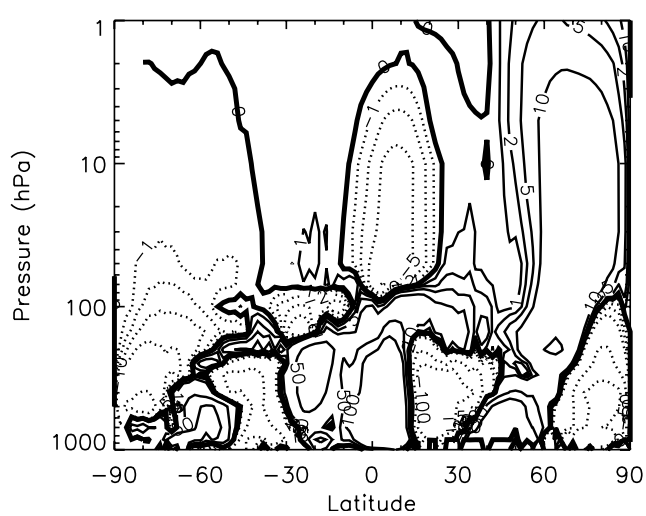

Figure 9. Decadal-mean difference of the DJF residual circulation. Positive values (solid lines) indicate increased circulation in the clockwise direction and vice versa for the negative contours (dashed lines).

simulate an atmosphere with increased CO_2. Using this specification, *Eichelberger and Hartmann*'s [2005] tropospheric temperature gradient resembled the SST-forced gradient in Run O. Similarly, they found that the extratropical stratosphere became warmer while the tropical stratosphere cooled. *Rind et al.* [1998] also note comparable stratospheric temperature differences solely due to dynamics. Interpretation of these results indicates that the GHG radiative cooling is greater than the SST-induced increased dynamical warming in the upper stratosphere.

[25] In the present study we show that the extratropical STE is linked to the changes in stratospheric wave driving and the residual circulation. While it is conceivable that changes in the stratospheric circulation may not always result in changes to the STE, the converse cannot be true. Any long-term trend in the annual extratropical STE must be accompanied by a change somewhere in the stratospheric circulation. Thus the annual STE provides a single-valued quantity related to the stratospheric circulation. Although it does not provide details of how or where the circulation changes, any increasing trend in the STE indicates some change in the Brewer-Dobson circulation. These changes could include a stronger tropical upwelling resulting in more meridional transport somewhere in the stratosphere or a broadening of the tropical upwelling region.

[26] Related to the magnitude of STE, we examine how the STE trend impacts how fast the mass and chemical species are transported through the upper troposphere/lower stratosphere. A characteristic residence time may be defined as the annual mean mass of the lowermost stratosphere between the tropopause and the 380 K surface divided by the rate of STE. We, again, note here that there is no significant trend evident in the annual mean mass of the lowermost stratosphere in our simulation. The mean mass of the lowermost stratosphere is 1.44×10^{17} kg and 1.49×10^{17} kg in the NH and SH, respectively. Using the beginning and end values to the best fit of the STE (Figure 2), our results show that the residence time in the NH decreases from 0.68 years at the beginning of the simulation to 0.60 years at the end, about a 12% difference. In the SH the residence time decreases from 0.80 to 0.73 years. The flux out the lowermost stratosphere increases with time, as does the stratospheric residual circulation. Thus the stratospheric mean age of air should trend younger. This is confirmed by chemical tracer analysis of CTM simulations driven with the GCM meteorological fields that shows the stratosphere is indeed younger at the end of Run O.

5. Summary and Conclusion

[27] We have examined the results from a 50-year integration of the GEOS-4 GCM that uses observed SSTs at the lower boundary. The GHG boundary conditions are held constant. We find that changes in the observed SSTs significantly alter the general circulation and temperature structure in the troposphere and stratosphere. Warmer temperatures in the tropical upper troposphere increase the subtropical temperature gradient. The local zonal mean flow in the subtropical upper troposphere/lower stratosphere increases accordingly. Vertically propagating waves from the troposphere to the stratosphere are refracted more poleward resulting in greater wave dissipation and forcing in the polar stratosphere. These changes are greatest in the upper stratosphere where the meridional residual circulation becomes stronger producing more stratospheric descent in the polar region.

[28] The trend in the stratospheric circulation and wave driving is reflected in an increasing trend of the extratropical STE. The magnitude of the annual STE is a convenient single-valued quantity related to changes in the stratospheric residual circulation. In particular, we find the NH STE is significantly correlated with the stratospheric wave forcing during DJF but not in other seasons. In other words, only the wave driving during winter significantly impacts the magnitude of the annual STE. We also note that as the rate of transport through the extratropical tropopause increases, the residence time of the air mass in the lowermost stratosphere decreases accordingly. The characteristic residence time decreases by about a month over the time span of our simulation.

[29] The magnitude of the STE trend and strengthening of the Brewer-Dobson circulation from the SST forcing alone is similar to results of earlier studies that explicitly include an increased GHG burden. Although these other climate studies vary considerably in the details of the response of the stratospheric circulation and dynamics, they all show a strengthening of the Brewer-Dobson circulation under conditions of a greater GHG burden. Results from another simulation identical to the SST-only experiment but with a trend in the GHG burden are examined in comparison. The STE trends and tropospheric temperature response in the increasing GHG simulation are not significantly different from the SST-only results. This indicates that the indirect SST mechanism is a significant process by which the GHG burden influences the residual circulation and STE. In contrast to the SST-only forcing in the present study, previous studies [*Rind et al.*, 1990; *Butchart and Scaife*, 2001; *Sigmond et al.*, 2004; *Butchart et al.*, 2006] and our increasing GHG simulation agree that GHG forcing results in a globally cooler stratosphere. Thus the stratospheric cooling from the GHGs is greater in magnitude than the increased dynamical warming.

[30] Finally, the SST boundary conditions have a large impact on the general atmospheric circulation and structure in the model. The SSTs will also impact the distribution of chemical species in the troposphere and stratosphere through these changes. By extension, and perhaps most importantly, these results also illustrate that simulations of 21st century stratosphere and climate using GCMs without interactive ocean layers are strongly dependant on the SSTs that are specified. Likewise, the stratospheric climate in coupled ocean-atmosphere models will be impacted by the accuracy of the modeled interface.

[31] **Acknowledgments.** We would like to thank three anonymous reviewers for their helpful comments and suggestions for improving this manuscript. This work was supported by NASA's EOS IDS and ACMAP programs.

References

Andrews, D. G., J. R. Holton, and C. B. Leovy (1987), *Middle Atmosphere Dynamics*, 489 pp., Academic, San Diego, Calif.

Appenzeller, C., J. R. Holton, and K. H. Rosenlof (1996), Seasonal variation of mass transport across the tropopause, *J. Geophys. Res.*, *101*, 15,071–15,078.

Bloom, S., et al. (2005), Documentation and validation of the Goddard Earth Observing System (GEOS) data assimilation system, version 4, *NASA Tech. Memo.*, *TM–2005–104606*, 187 pp.

Brewer, A. M. (1949), Evidence for a world circulation provided by the measurements of helium and water vapor distribution in the stratosphere, *Q. J. R. Meteorol. Soc.*, *75*, 351–363.

Butchart, N., and A. A. Scaife (2001), Removal of chlorofluorocarbons by increased mass exchange between the stratosphere and troposphere in a changing climate, *Nature*, *410*, 799–802.

Butchart, N., et al. (2006), Simulations of anthropogenic change in the strength of the Brewer-Dobson circulation, *Clim. Dyn.*, *27*, 727–741, doi:10.1007/s00382-006-0162-4.

Dobson, G. M. B. (1956), Origin and distribution of polyatomic molecules in the atmosphere, *Proc. R. Soc. London Ser. A*, *236*, 187–193.

Douglass, A. R., M. R. Schoeberl, R. B. Rood, and S. Pawson (2003), Evaluation of transport in the lower tropical stratosphere in a global chemistry and transport model, *J. Geophys. Res.*, *108*(D9), 4259, doi:10.1029/2002JD002696.

Eichelberger, S. J., and D. L. Hartmann (2005), Changes in the strength of the Brewer-Dobson circulation in a simple AGCM, *Geophys. Res. Lett.*, *32*, L15807, doi:10.1029/2005GL022924.

Grassi, B., G. Redaelli, and G. Visconti (2005), Simulation of Polar Antarctic trends: Influence of tropical SST, *Geophys. Res. Lett.*, *32*, L23806, doi:10.1029/2005GL023804.

Haynes, P. H., M. E. McIntyre, T. G. Sheperd, C. J. Marks, and K. P. Shine (1991), On the "downward control" principle of extratropical circulations by eddy-induced mean zonal forces, *J. Atmos. Sci.*, *48*, 651–678.

Haywood, J. M., M. D. Schwartzkopf, and V. Ramaswamy (1998), Estimates of radiative forcing due to modeled increases in tropospheric ozone, *J. Geophys. Res.*, *103*, 16,999–17,007.

Hoerling, M. P., J. W. Hurrell, and T. Xu (2001), Tropical origins for recent North Atlantic climate change, *Science*, *292*, 90–92.

Holton, J. R., P. H. Haynes, M. E. McIntyre, A. R. Douglass, R. B. Rood, and L. Pfister (1995), Stratosphere-troposphere exchange, *Rev. Geophys.*, *33*, 403–439.

Hoskins, B. J. (1991), Toward a PV-theta view of the general circulation, *Tellus Ser. A*, *43*, 27–35.

Knutson, T. R., and S. Manabe (1998), Model assessment of decadal variability and trends in the tropical Pacific Ocean, *J. Clim.*, *11*, 2273–2296.

Knutson, T. R., T. L. Delworth, K. W. Dixon, and R. J. Stouffer (1999), Model assessment of regional surface temperature trends (1949–1997), *J. Geophys. Res.*, *104*, 30,981–30,996.

Langematz, U., M. Kunze, K. Krüger, K. Labitzke, and G. L. Roff (2003), Thermal and dynamical changes of the stratosphere since 1979 and their link to ozone and CO_2 changes, *J. Geophys. Res.*, *108*(D1), 4027, doi:10.1029/2002JD002069.

Levy, H., II (1971), Normal atmosphere: Large radical and formaldehyde concentrations predicted, *Science*, *173*, 141–143.

Mahfouf, J. F., D. Cariolle, J.-F. Royer, J.-F. Geleyn, and B. Timbal (1994), Response of the Meteo-France climate model to changes in CO_2 and sea surface temperature, *Clim. Dyn.*, *9*, 345–362.

Olsen, M. A., M. R. Schoeberl, and A. R. Douglass (2004), Stratosphere-troposphere exchange of mass and ozone, *J. Geophys. Res.*, *109*, D24114, doi:10.1029/2004JD005186.

Olsen, M. A., A. R. Douglass, R. S. Stolarski, and M. R. Schoeberl (2006), On detecting a trend in the residual circulation from observations of column HCl, *Geophys. Res. Lett.*, *33*, L14815, doi:10.1029/2006GL026214.

Rayner, N. A., D. E. Parker, E. B. Horton, C. K. Folland, L. V. Alexander, D. P. Rowell, E. C. Kent, and A. Kaplan (2003), Global analyses of sea surface temperature, sea ice, and night marine air temperature since the late nineteenth century, *J. Geophys. Res.*, *108*(D14), 4407, doi:10.1029/2002JD002670.

Rind, D., R. Suozzo, N. K. Balachandran, and M. J. Prather (1990), Climate change and the middle atmosphere. part I: The doubled CO_2 climate, *J. Atmos. Sci.*, *47*, 475–494.

Rind, D., D. Shindell, P. Lonergan, and N. K. Balachandran (1998), Climate change and the middle atmosphere. part III: The doubled CO_2 climate revisited, *J. Clim.*, *11*, 876–894.

Schoeberl, M. R. (2004), Extratropical stratosphere-troposphere mass exchange, *J. Geophys. Res.*, *109*, D13303, doi:10.1029/2004JD004525.

Schoeberl, M. R., A. R. Douglass, Z. Zhu, and S. Pawson (2003), A comparison of the lower stratospheric age spectra derived from a general circulation model and two data assimilation systems, *J. Geophys. Res.*, *108*(D3), 4113, doi:10.1029/2002JD002652.

Sigmond, M., P. C. Siegmund, E. Manzini, and H. Kelder (2004), A simulation of the separate climate effects of middle-atmospheric and tropospheric CO_2 doubling, *J. Clim.*, *17*, 2352–2367.

Stolarski, R. S., A. R. Douglass, S. Steenrod, and S. Pawson (2006), Trends in stratospheric ozone: Lessons learned from a 3D chemical transport model, *J. Atmos. Sci.*, *63*, 1028–1041.

M. A. Olsen, Goddard Earth Sciences and Technology Center, University of Maryland Baltimore County, 5523 Research Park Drive, Suite 320, Baltimore, MD 21228, USA. (olsen@hyperion.gsfc.nasa.gov)

M. R. Schoeberl, NASA Goddard Space Flight Center, Greenbelt, MD 20771, USA.

J. E. Nielsen, Science Systems and Applications, Inc., 10210 Greenbelt Road, Suite 600 Lanham, MD 20706, USA.